J Ginseng Res 43 (2019) 272–281

Contents lists available at ScienceDirect

Journal of Ginseng Research

journal homepage: http://www.ginsengres.org

Research Article

Panax ginseng (Korea Red Ginseng) repairs diabetic sensorineural damage through promotion of the nerve growth factor pathway in diabetic zebrafish

Youn Hee Nam [1,☆], Hyo Won Moon [1,☆], Yeong Ro Lee [1], Eun Young Kim [1], Isabel Rodriguez [1], Seo Yule Jeong [1], Rodrigo Castañeda [1], Ji-Ho Park [2], Se-Young Choung [3], Bin Na Hong [1], Tong Ho Kang [1,*]

[1] *Department of Oriental Medicine Biotechnology, College of Life Sciences and Graduate School of Biotechnology, Kyung Hee University, Global Campus, Gyeonggi, Republic of Korea*
[2] *Graduate School of East-West Medical Science, Kyung Hee University, Global Campus, Gyeonggi, Republic of Korea*
[3] *Department of Preventive Pharmacy and Toxicology, College of Pharmacy, Kyung Hee University, Seoul, Republic of Korea*

ARTICLE INFO

Article history:
Received 5 September 2017
Received in Revised form
31 January 2018
Accepted 12 February 2018
Available online 16 February 2018

Keywords:
Alloxan
Diabetic sensorineural damage
Neuromast
Red ginseng
Zebrafish

ABSTRACT

Background: Diabetic sensorineural damage is a complication of the sensory neural system, resulting from long-term hyperglycemia. Red ginseng (RG) has shown efficacy for treatment of various diseases, including diabetes mellitus; however, there is little research about its benefit for treating sensorineural damage. Therefore, we aim to evaluate RG efficacy in alloxan-induced diabetic neuromast (AIDN) zebrafish.
Methods: In this study, we developed and validated an AIDN zebrafish model. To assess RG effectiveness, we observed morphological changes in live neuromast zebrafish. Also, zebrafish has been observed to have an ultrastructure of hair-cell cilia under scanning electron microscopy. Thus, we recorded these physiological traits to assess hair cell function. Finally, we confirmed that RG promoted neuromast recovery via nerve growth factor signaling pathway markers.
Results: First, we established an AIDN zebrafish model. Using this model, we showed via live neuromast imaging that RG fostered recovery of sensorineural damage. Damaged hair cell cilia were recovered in AIDN zebrafish. Furthermore, RG rescued damaged hair cell function through cell membrane ion balance.
Conclusion: Our data suggest that RG potentially facilitates recovery in AIDN zebrafish, and its mechanism seems to be promotion of the nerve growth factor pathway through increased expression of topomyosin receptor kinase A, transient receptor potential channel vanilloid subfamily type 1, and mitogen-activated protein kinase phosphorylation.

1. Introduction

Panax ginseng has been use for thousands of years in Asian countries for diabetic therapy. Red ginseng (RG) is prepared by steaming the roots of *P. ginseng*. RG and its ginsenosides have broad pharmacological values, including anticancer [1], antiinflammatory [2], and antidiabetic properties [3], as well as the ability to improve chronic liver disease [4]. However, little is known about the potential efficacy of RG for the diabetic sensorineural system.

Neuromasts located at the surface from the head to the trunk of fish and aquatic amphibians are considered sensory organs [5]. Owing to their physical location, neuromasts are easily visualized [6]. Neuromasts are able to detect and localize water movement around the body and are implicated in several behaviors [7]. Each neuromast is composed of a central core of hair cells surrounded by progenitor cells and mantle cells, which are supporting cells. Neuromasts are innervated by the peripheral projections of afferent neurons located in the posterior lateral line ganglion [8–11]. In our model, the zebrafish peripheral nerve was damaged by diabetic sensorineural damage. Hyperglycemia induces oxidative stress, which is the underlying cause of development and progression of diabetic sensorineural damage, an important complication of diabetes [12–14].

* Corresponding author. Graduate School of Biotechnology, Department of Oriental Medicine Biotechnology, Kyung Hee University, 1732, Deogyeong-daero, Giheung-gu, Yongin-si, Gyeonggi-do, 17104, Republic of Korea.
E-mail address: panjae@khu.ac.kr (T.H. Kang).
☆ The first two authors contributed equally to this work.

https://doi.org/10.1016/j.jgr.2018.02.006
p1226-8453 e2093-4947/$ – see front matter

Nerve growth factor (NGF) is among the most important molecular targets of diabetic peripheral neuropathy, reduced levels or activity of NGF play a key role in diabetic neuropathy pathogenesis [31,32]. There are two NGF receptors, p75 neurotrophin receptor (p75NTR) with low affinity and tropomyosin receptor kinase (Trk) with high affinity for NGF, which are expressed in the peripheral nervous system [33]. Moreover, NGF is associated with modulation of transient receptor potential channel vanilloid subfamily type 1 (TRPV1) expression [26,34], which is well known to cause a sensation of scalding heat and pain during peripheral neuropathy [30]. Therefore, we aimed to evaluate RG efficacy for alloxan-induced diabetic sensorineural damage zebrafish and to investigate the underlying mechanisms. Thus, we investigated the role of RG in trkA and TRPV1 expression and in the downstream of the NGF pathway through mitogen-activated protein kinase (MAPK) level.

Consequently, we established an alloxan-induced diabetic neuromast (AIDN) zebrafish model and then evaluated recovery due to RG through observation of live neuromasts. The ultrastructure of hair cell cilia in RG-treated zebrafish was observed under scanning electron microscopy (SEM), and we performed physiological recordings to assess hair cell function. Finally, we confirmed RG-promoted neuromast recovery via NGF signaling pathway markers.

2. Materials and methods

2.1. Reagents and equipment

Alloxan monohydrate, sea salt, tricaine methanesulfonate, and tert-butanol were purchased from Sigma Chemical Co. (St. Louis, MO, USA). 2-(N-(7-nitrobenz-2-oxa-1,3-diazol-4-yl) amino)-2-deoxyglucose (2-NBDG) and YO-PRO were purchased from Invitrogen (Life Technologies, Grand Island, NY, USA). An Olympus 1×70 microscope was used for fluorescence microscopy (Olympus, Japan). Focus Lite (Focus Co, Daejeon, Korea) and Image J software (National Institutes of Health, Bethesda, MD, USA) were used for image analyses. Red ginseng extract was obtained from the Korea Ginseng Corporation (Taejon, Korea). The Korean Red Ginseng extract used in this study (crude saponin 70 mg/g, solid component 60%, or more) contained Rb1 (0.46%), Rb2 (0.23%), Rc (0.28%), Rd (0.09%), Re (0.12%), Rf (0.10%), Rg1 (0.07%), Rg2 (0.14%), Rg3 (0.12%), Rh1 (0.10%), and other minor ginsenosides.

2.2. Zebrafish maintenance

Adult zebrafish (wild-type) were maintained in an aquarium with a continuous recirculating system. Fish were fed commercially available fish food and newly hatched brine shrimp twice a day. Three sexually mature female and three sexually mature male zebrafish were allowed to breed in a breeding cage at night. The next morning, the embryos were placed at the bottom of the breeding cage and collected 2 hours postfertilization. The embryos were separated and raised in 0.03% sea salt solution in a Petri dish. Zebrafish embryos were maintained in a 14-hour light/10-hour dark photoperiod at 28°C. Fish were cared for in accordance with standard zebrafish protocols approved by the Animal Care and Use Committee of the Kyung Hee University (KHUASP(SE)-15-10).

2.3. Validation of alloxan to confirm the extent of neuromast damage

Five days postfertilization (dpf), wild-type zebrafish larvae were placed into 96-well plates. The zebrafish larvae were treated with various concentrations of alloxan (100, 300, 500, and 700 μM) for 2 days and for 4 days, respectively. Afterward, each zebrafish was rinsed three times with 0.03% sea salt solution. The lateral line neuromasts were labeled using 0.1% YO-PRO for 30 minutes. YO-PRO is a cyanine dye that selectively binds to DNA so that each hair cell nuclei is stained. Larvae were washed using 0.03% sea salt solution and then anesthetized using 0.004% tricaine solution. The number of green fluorescent-labeled neuromasts was counted under fluorescence microscopy.

2.4. Alloxan toxicity test

Twenty zebrafish embryos were used for the toxicity test of alloxan. Embryos were placed in 6-well plates and incubated at 28.5°C under a 14-hour light/10-hour dark photoperiod. Four treatments were used: alloxan at 0-μM, 100-μM, 300-μM, or 500-μM concentration. The embryos were observed under microscopy 2 days after treatment, and heartbeat and hatching rate were recorded.

2.5. Evaluation of live neuromasts by RG on AIDN zebrafish

Five dpf, wild-type zebrafish larvae were exposed to 300-μM concentrations of alloxan for 72 hours in a 96-well plate. Following alloxan treatment, the larvae were treated with 50 μg/mL or 100 μg/mL of RG extract for 12 hours. Afterward, each zebrafish was rinsed in 0.03% sea salt solution. Neuromast hair cells were stained with 0.1% YO-PRO for 30 minutes. The total number of lateral line neuromasts was counted under fluorescence microscopy. Additionally, changes in pancreatic islet β-cells after alloxan exposure were assessed using the method described above.

2.6. SEM observation of hair cell cilia in AIDN zebrafish

SEM was used to investigate the loss or recovery of hair cell cilia. Zebrafish larvae from each group were fixed for 12 hours in 2.5% glutaraldehyde in phosphate buffered saline at 4°C. Larvae were washed three times for 5 minutes in distilled water and then were dehydrated through serial exposure to graded concentrations of ethanol solution (25%, 50%, 70%, 80%, 95%, and 100%) for 10 minutes. Next, zebrafish larvae samples were dehydrated through serial exposure to graded concentration of tert-butanol in ethanol (25%, 50%, 75%, and 100%) for 10 minutes. Finally, the specimens were dried using a critical point dryer and were sputter-coated twice with platinum using an ion sputter coater (ps-1200; Tescan, Czech Republic). The hair cell cilia were observed using SEM (supra55; Zeiss, Germany) at 10 kV.

2.7. Evaluation of hair cell function using physiological recordings of AIDN zebrafish

Five dpf, larvae were exposed to alloxan and then treated with RG as described above. Each larva was placed in a silicone Sylgard-coated cell dish containing extracellular solutions (134 mM NaCl, 2.9 mM KCl, 1.2 mM $MgCl_2$, 2.1 mM $CaCl_2$, 10 mM glucose, 10 mM HEPES buffer, adjusted to a pH of 7.8 with NaOH). Each larva was anesthetized in embryo media containing 0.004% tricaine for 30 seconds. The larvae were positioned laterally and mounted with Vaseline. One point was just posterior to the bladder, and the other point was near the tail end of the larva. To record neuromast activity, larvae were immobilized with the 0.004% tricaine. Each neuromast's condition was checked under fluorescence microscopy, and the posterior trunk L1 neuromast resting membrane potential signal was measured with a microelectrode. The microelectrode was filled with 3 M KCl, and the electrode resistance was set to range between 5 and 10 M Ω in extracellular solution. Recorded values were converted to digital signals with AXOCLAMP-2B.

2.8. Pancreatic islet recovery by RG on AIDN zebrafish

Five dpf, wild-type zebrafish larvae were exposed to 300 μM of alloxan for 72 hours in a 96-well plate. Following alloxan treatment, the larvae were treated with 100 μg/mL of RG extract for 12 hours. RG-treated zebrafish larvae were exposed to 25 μM of 2-NBDG for 12 hours, and then pancreatic islets were imaged by fluorescence microscopy. Damaged β-cell regeneration due to the effect of RG was confirmed in the *ins*:GFP line zebrafish based on green fluorescence protein tagging in the β-cells. Transgenic zebrafish lines expressing GFP specifically in β-cells were obtained from the Zebrafish Organogenesis Mutant Bank. Pancreatic islets and β-cells were analyzed using Focus Lite software or Image J software.

2.9. Total RNA isolation

Total RNA was isolated from zebrafish larvae using Trizol reagent (Life science) following the manufacturer's instructions. For this, 500 μL of Trizol reagent was added to whole larva samples and then the samples were homogenized. Total RNA was separated from the sample using chloroform containing amylenes (Sigma-Aldrich) and centrifugation. This was followed by treatment with 99.5% isopropanol (Samchun Chemical) and another round of centrifugation. Finally, the sample was washed with 75% EtOH and diethyl pyrocarbonate-treated water, and the total RNA sample was dissolved in diethyl pyrocarbonate water. The remaining amount of RNA was measured with a NanoDrop 2000 (Thermo Scientific).

2.10. cDNA synthesis

Genomic DNA was removed from the total RNA sample using DNase I (Promega) at 37°C on a heat block for 30 minutes (thermoBATH). Next, cDNA was synthesized from 4 mg of total RNA using the RevertAid First Strand cDNA Synthesis Kit (Thermo Scientific) and Oligo(dT)$_{18}$ primer, following the manufacturer's instructions.

2.11. Quantitative real-time polymerase chain reaction (RT-PCR)

Changes in candidate mRNA levels in the zebrafish fries were identified by real-time RT PCR using SYBR Green Master mix (Applied Biosystems) with the primers listed in Table 1. Real-time PCR conditions consisted of one cycle of 5 minutes at 95°C; followed by 45 cycles of (1) 95°C for 15 seconds, (2) 60°C for 15 seconds, and (3) 72°C for 30 seconds; and, lastly, one cycle of 10 minutes at 72°C. Each real-time PCR was carried out in triplicate in a total reaction mixture of 10 μL using a Rotor gene 6000 (Qiagen). The housekeeping gene β-actin was concurrently amplified in each sample as a control and was used for normalization. Finally, real-time PCR results were calculated using the $-2^{\Delta\Delta Ct}$ method [15].

2.12. Protein extraction

Whole larvae were extracted via homogenization in 300 μl of cold extraction buffer (HEPES 20 mM, KCl 100 mM, glycerol 5%, EDTA 5 mM, $MgCl_2$ 1 mM, DTT 1 mM, Triton X-100 0.1%) with protease inhibitors (Roche). Next, the samples were centrifuged at 14,000 rpm at 4°C for 15 minutes. Protein levels were measured using the NanoDrop 2000 (Thermo Scientific).

2.13. Western blot

Total protein was loaded into the sodium dodecyl sulfate polyacrylamide gel electrophoresis (SDS-PAGE) and subsequently transferred to a nitrocellulose membrane (Millipore). The membrane was blocked with 5% skim milk (Bio Basic Canada Ins.) in tris-buffered saline with Tween 20 (TBS-T) (137 mM of sodium chloride, 20 mM Tris, 0.1% Tween 20, supplied at pH 7.6). After the blocking step, the membrane was probed with an anti-p-MAPK (Cell Signaling, 1:2000), α-tubulin (EPICMICS, 1:1000), and primary antibody. MAPK phosphorylation (p-MAPK) was normalized by α-tubulin, followed by the addition of horseradish peroxidase-conjugated anti-rabbit secondary antibody (Bethyl, 1:5000). Immunoreactive proteins were visualized using a WEST-One (iNtRON) and an ImageQuant™ LAS 4000 (GE Healthcare). Band intensities were determined using Quantity One software (Bio-Rad).

2.14. Statistical analysis

Statistical analysis was performed using GraphPad Prism (version 5). All data are expressed as mean ± standard error of the mean. Significance was determined using one-way analysis of variance followed by Tukey's test. The probability level for statistical significance was set at $p < 0.05$.

3. Results

3.1. Optimization of alloxan for neuromast damage in zebrafish

This study was designed to produce alloxan-induced neuromast damage in zebrafish. We confirmed the extent of neuromast damage caused by alloxan. As shown in Fig. 1A, alloxan concentration was validated in five-dpf zebrafish larvae. The trunk neuromasts (Fig. 1B) were analyzed for damage by alloxan after 2 days and 4 days of exposure to various doses (100 μM, 300 μM, and 500 μM). Two days and 4 days after alloxan treatment, the trunk neuromasts decreased in a dose- and time-dependent manner (Fig. 1 C, D). Normal zebrafish were observed to have 19.3 ± 1.0 neuromasts, while after two days, the 100-μM, 300-μM, and

Table 1
Primer sequences for real-time RT-PCR

Gene	Strand	Sequence (5′-3′)	Gene bank accession number
TrkA (tyrosine kinase receptor)	Forward	ACT CCA AGT TTG GCA TCC AC	JN_837101.1
	Reverse	GGG TTC TCC ACA AAA CTG GA	
PEPCK (phosphoenolpyruvate carboxykinase)	Forward	GAA CCT CCA GCA AAA CCA CA	NM_214751.1
	Reverse	GTC AGC GTC ACT CCT TCA G	
Trpv1 (transient receptor potential cation channel, subfamily V, member 1)	Forward	TCC AAC CCT CAA AGT CGT ATG	XM_005165327.2
	Reverse	TCA ATC CAA ATC GTC CCC TG	
β-Actin	Forward	CAAGCAGGAGTACGATGAGTC	NM_181601.4
	Reverse	GTC GTT TGA AGT TTC TCT GCG	

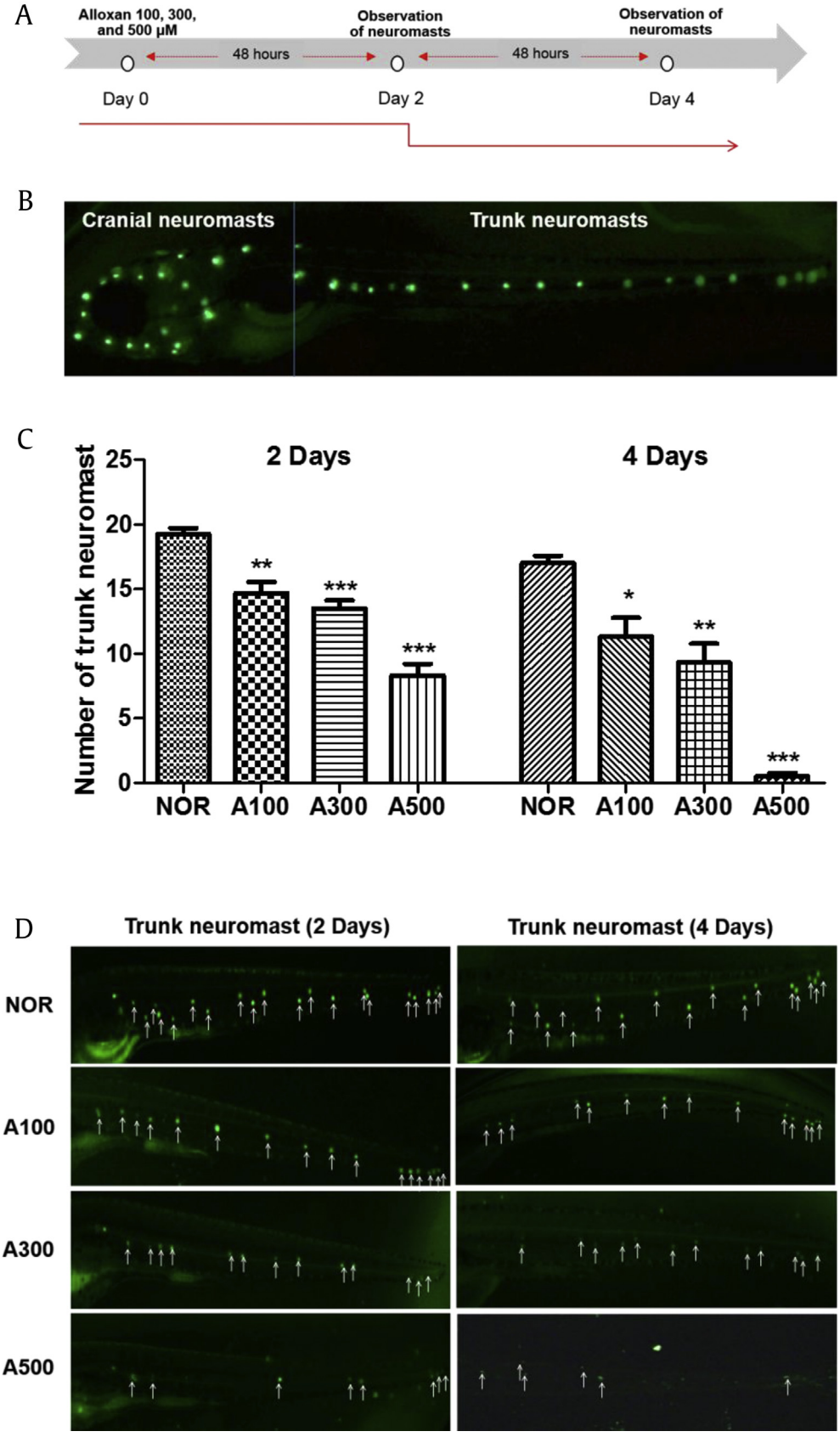

Fig. 1. (A) Scheme of experiment. (B) Lateral line for zebrafish. (C) Number of trunk neuromasts of alloxan dose-dependently damaged zebrafish. (D) Fluorescent microscopic image of trunk neuromast following treatment with 0.1 YO-PRO ($^{*}p < 0.05$, $^{**}p < 0.01$, $^{***}p < 0.001$; compared to normal (NOR) zebrafish).

500-μM alloxan-treated zebrafish had significantly fewer neuromasts: 14.7 ± 1.5 ($p = 0.0044$), 13.5 ± 1.3 ($p = 0.0004$), and 8.3 ± 1.5 ($p < 0.001$), respectively. After 4 days, normal zebrafish were observed to have an average of 17.0 ± 1.0 neuromasts. The 100-μM, 300-μM, and 500-μM alloxan-treated zebrafish had significantly fewer neuromasts: 11.3 ± 2.5 ($p = 0.0223$), 9.3 ± 2.5 ($p = 0.0080$), and 0.5 ± 0.6 ($p < 0.001$), respectively.

3.2. Evaluation of otic 1 hair cell (O1), lateral neuromast 1 (L1), lateral neuromast 4 (L4), and terminal neuromast (T) parts on AIDN zebrafish

To evaluate O1, L1, L4 neuromasts, and T damage in neuromasts after alloxan-induced damage in zebrafish, we observed each part after 2 days and found days using 0.1% YO-PRO. As shown (Fig. 2A),

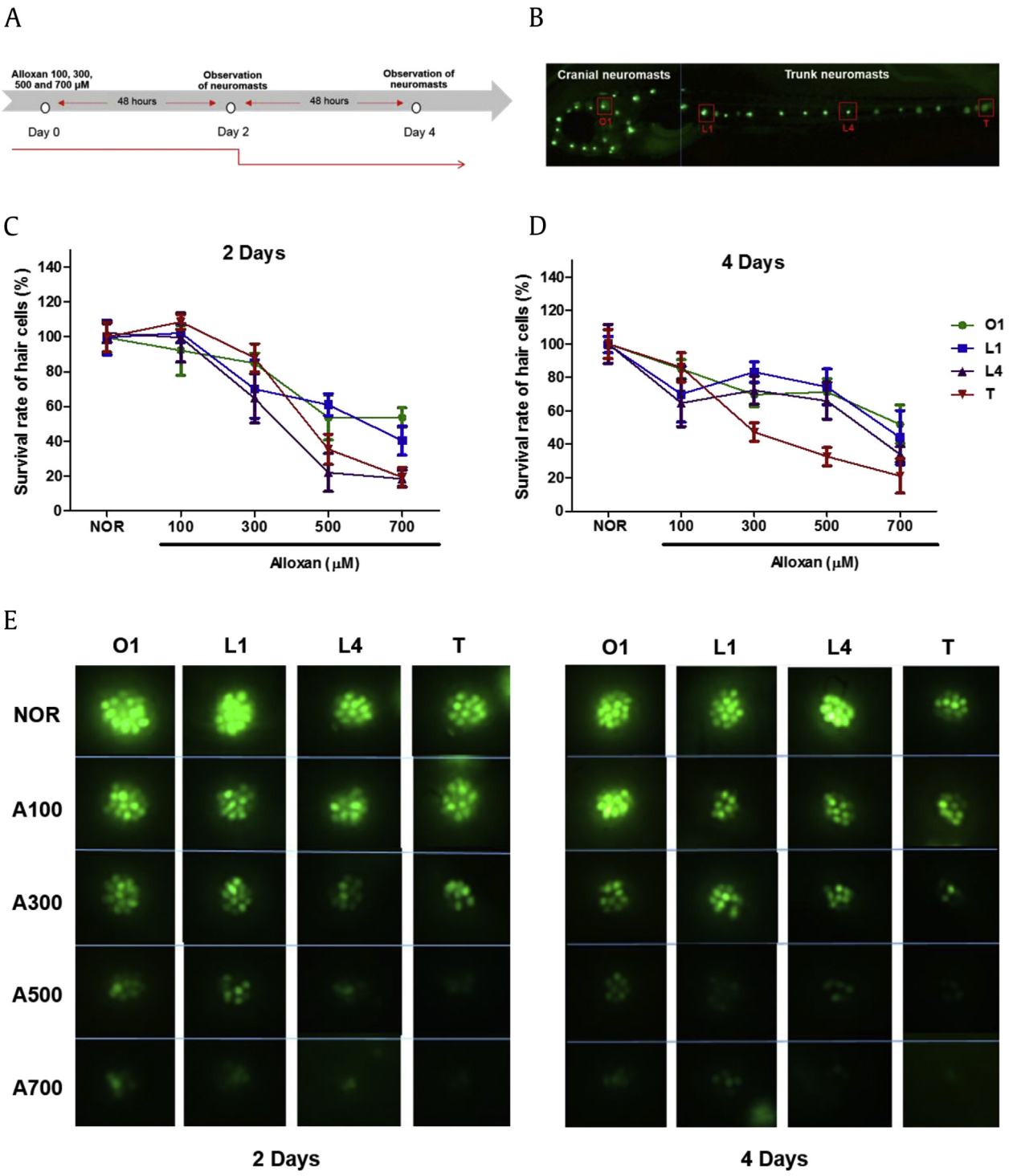

Fig. 2. (A) Scheme of experiment. (B) The otic 1 hair cell in cranial neuromasts, lateral neuromasts 1 and 4, and terminal neuromasts in zebrafish. (C) The survival rate of each hair cell of alloxan dose-dependently damaged zebrafish following 2 days of treatment. (D) The survival rate of each hair cell type in alloxan dose-dependently damaged zebrafish following 4 days of treatment. (E) Fluorescent microscopic image of each hair cell type following 0.1% YO-PRO treatment.
O1, otic 1 hair cell; L1, lateral neuromast 1; L4, lateral neuromast 4; T, terminal neuromast.

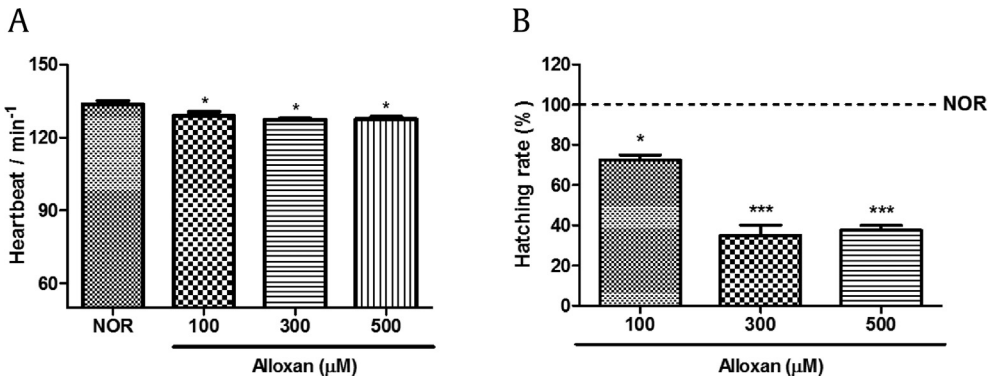

Fig. 3. Toxicity of alloxan in zebrafish embryos. (A) Heartbeat per minute in zebrafish exposed to alloxan for 48 hours. (B) Hatching rate in zebrafish exposed to alloxan for 48 hours ($^{*}p < 0.05$, $^{***}p < 0.001$; compared to normal).

several alloxan concentrations were applied to five-dpf zebrafish larvae. The otic 1 hair cell in cranial neuromasts, lateral neuromasts 1 and 4, and terminal neuromasts in zebrafish (Fig. 2B) were analyzed for damage after 2 and 4 days of exposure to several alloxan doses (100 μM, 300 μM, 500 μM, and 700 μM). After 2 and 4 days alloxan treatment, O1, L1, L4, and T number were decreased in a dose- and time-dependent manner. The greatest damage was observed on the terminal part (Fig. 2C–E).

3.3. Alloxan toxicity test

To evaluate alloxan toxicity, we measured heartbeat and hatching rate. Alloxan-treated zebrafish had significantly decreased heartbeat compared with normal zebrafish (Fig. 3A). Furthermore, alloxan-treated zebrafish exhibited a dose-dependent decrease in hatching rate (Fig. 3B).

3.4. Recovery of live neuromasts by RG in AIDN zebrafish

To evaluate the efficacy of RG, we investigated trunk neuromasts after alloxan with RG at 50 μg/mL and 100 μg/mL doses. The normal group had 20.0 ± 0.6 neuromasts. The alloxan-treated group had significantly fewer neuromasts by 12.9 ± 1.8 ($p < 0.001$). The RG-treated group showed increased neuromast numbers compared with the alloxan-treated group. Specially, the 50 μg/mL and 100 μg/mL RG-treated groups showed significantly higher numbers by 16.0 ± 2.8 ($p = 0.0284$) and 17.4 ± 1.0 ($p < 0.001$), respectively (Fig. 4).

3.5. Effect of RG on hair cell cilia

To investigate the loss or recovery of cilia, we assessed the morphological differences of cilia among groups under SEM (Fig. 5). Each neuromast was composed of sensory hair cells with a covered cupula. Cilia bundles were observed in the normal group, whereas cilia bundles of hair cells were destroyed in specimens treated with 300 μM alloxan. However, cilia bundles from hair cells in larvae were recovered with the RG treatment (100 μg/mL).

3.6. Effect of RG on resting membrane potential of neuromast hair cells

The resting membrane potential of L1 hair cells was measured to investigate electrical activity using the physiological recording method. Resting membrane potential was defined as the membrane voltage measured by a current clamp with no applied current. The hair cells were accessible via microelectrode, and the resting membrane value was recorded easily (Fig. 6A). As a result, in the normal group, the mean value of resting membrane potential was −46 mV. The average resting membrane value of the alloxan-

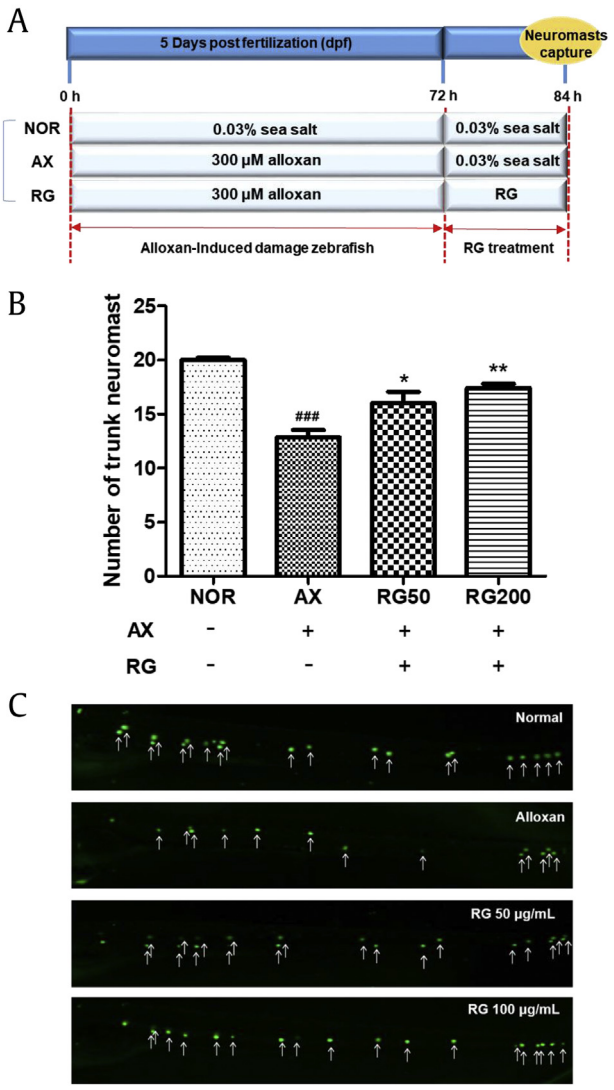

Fig. 4. (A) Scheme of experiment. (B) The number of trunk neuromasts in RG-treated AIDN zebrafish. (C) Fluorescent microscopic image of trunk neuromasts following treatment with 0.1% YO-PRO ($^{###}p < 0.001$; compared to normal), ($^{*}p < 0.05$, $^{**}p < 0.01$; compared to alloxan (AX)).
AIDN, alloxan-induced diabetic neuromast; RG, red ginseng.

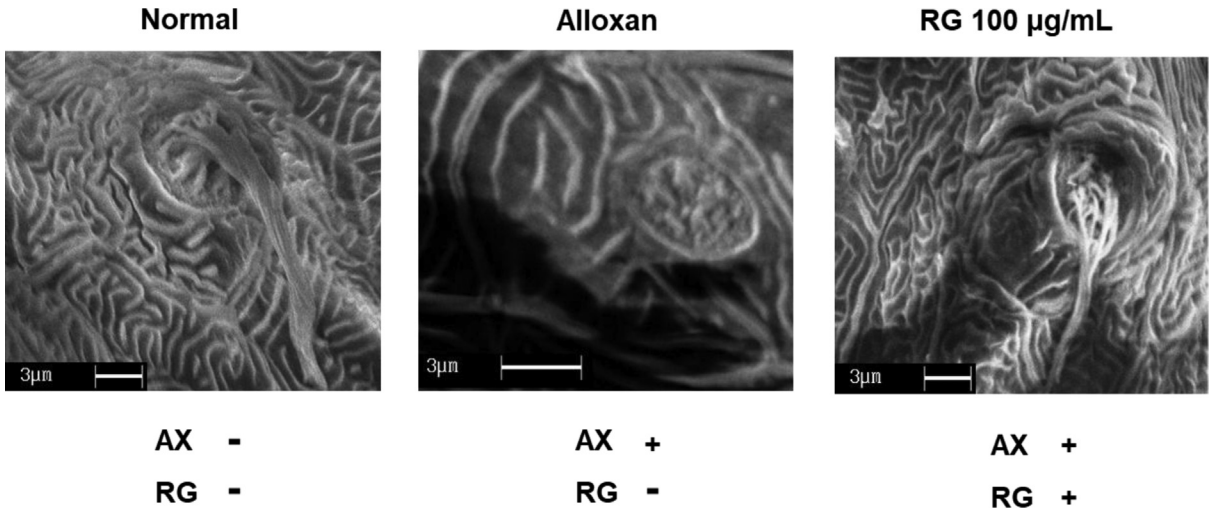

Fig. 5. Scanning electron microscopy (SEM) images of representative neuromasts in zebrafish larva. Scale bar = 3 μm.
RG, red ginseng.

treated group was significantly higher, up to −8 mV. Treatment with RG significantly decreased the resting membrane potential compared with the alloxan-treated group (Fig. 6B and C)

3.7. Effect of RG on pancreatic islet

Alloxan is a known diabetogenic chemical and is reported to decrease β-cell mass in the pancreatic islet. To investigate the pancreatic islet recovery rate according to RG presence, we used wild-type zebrafish stained with 2-NBDG dye and zebrafish from the Tg transgenic line (*ins*:GPF; transgenic zebrafish lines expressing GFP specifically in β-cells). The pancreatic islet size of the alloxan-treated group was significantly decreased by 74.6% compared to the normal group ($p = 0.0002$). In contrast, the islet size in 100-μg/ml RG-treated group increased significantly by 40.4% compared with the alloxan-treated group ($p = 0.0380$; Fig. 7A and B). Additionally, the alloxan-treated group was confirmed to damage β-cells compared with the normal group via the relative fluorescence intensity value. Damaged β-cells were repairable with the RG treatment (100 μg/mL) (Fig. 7C and D).

3.8. Phosphoenolpyruvate carboxykinase, TRPV1, and TrkA mRNA levels in AIDN zebrafish

Phosphoenolpyruvate carboxykinase (PEPCK) catalyzes gluconeogenesis and is regulated by glucagon and insulin [16]. The PEPCK expression level in the alloxan-treated group showed a tendency to increase when compared to the normal group, whereas the PEPCK mRNA level tends to decrease with RG exposure (Fig. 8A). While there are multiple peripheral and central neural

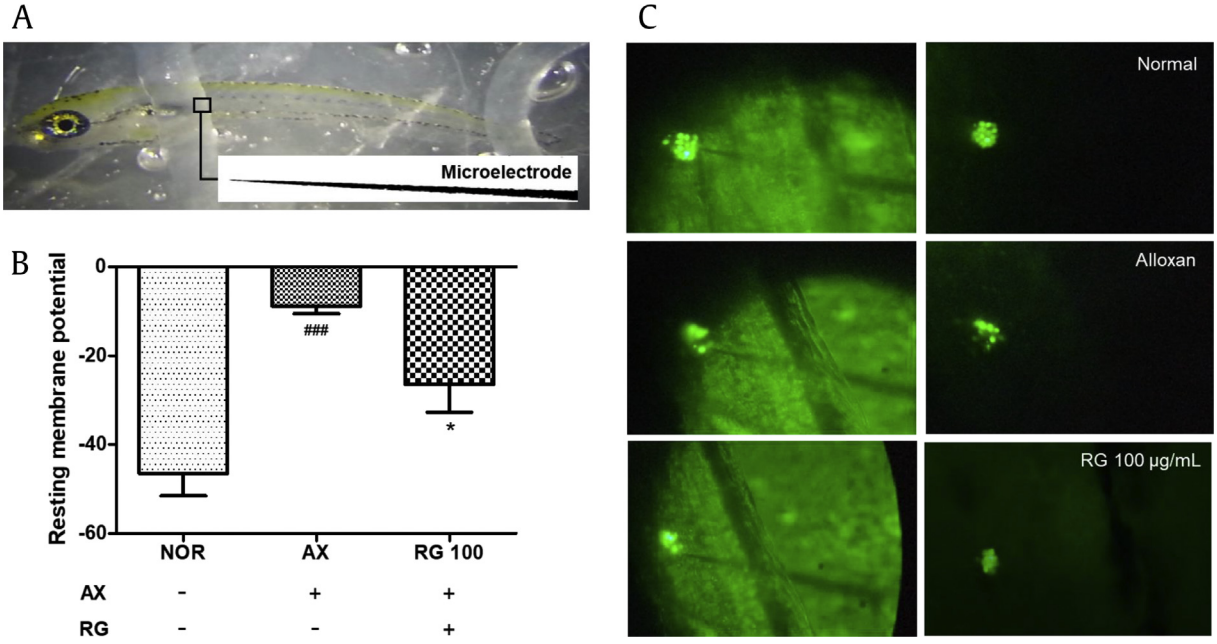

Fig. 6. Measure of resting membrane potential on an L1 neuromast. (A) Lateral mounting of zebrafish shows the location of the microelectrode in the L1 neuromast. (B) Value of resting membrane potential. (C) Image of an L1 neuromast ($^{###}p < 0.001$; compared to normal, $^{*}p < 0.05$; compared to alloxan treatment).
L1, lateral neuromast 1; RG, red ginseng.

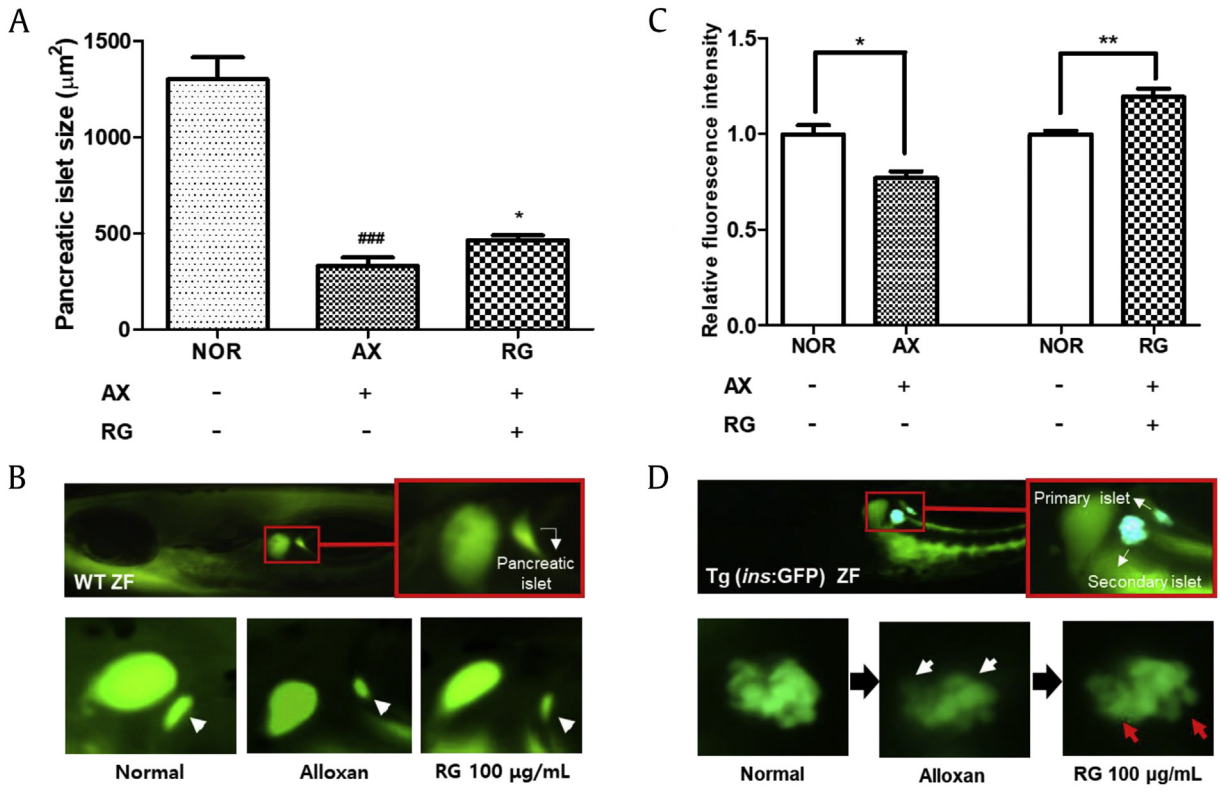

Fig. 7. Effect of RG on pancreatic islet. (A) Pancreatic islet size by RG. (B) Pancreatic islet image of each group. (C) Relative fluorescence intensity of pancreatic β-cells by RG. (D) Pancreatic β-cell image of each group ($^{###}p < 0.001$; compared to normal, $^{*}p < 0.05$; compared to alloxan treatment, $^{*}p < 0.05$, $^{**}p < 0.01$).
RG, red ginseng.

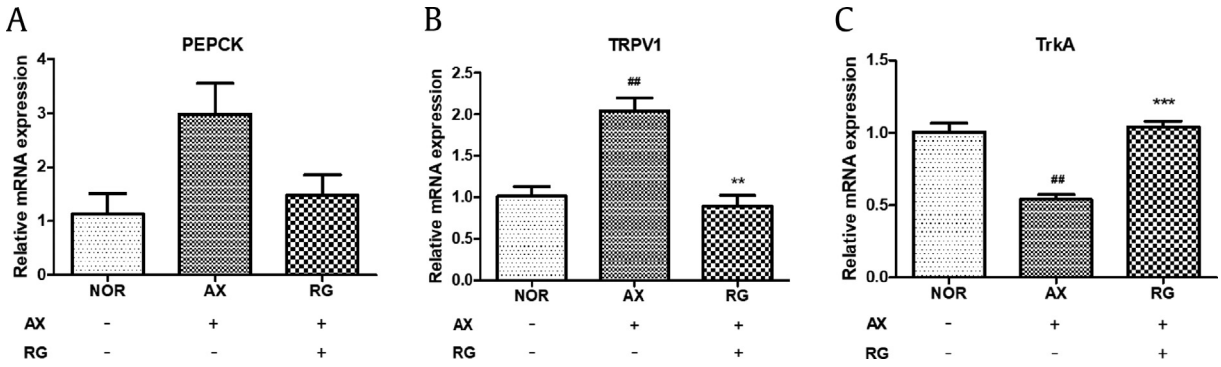

Fig. 8. Expression of PEPCK, TRPV1, and TrkA in AIDN zebrafish ($^{##}p < 0.01$; compared to normal, $^{**}p < 0.01$, $^{***}p < 0.001$; compared to alloxan treatment). (A) PEPCK expression. (B) TRPV1 expression. (C) TrkA expression.
AIDN, alloxan-induced diabetic neuromast; PEPCK, phosphoenolpyruvate carboxykinase; TRPV1, transient receptor potential channel vanilloid subfamily type 1; TrkA, topomyosin receptor kinase A.

mechanisms of NGF-TrkA-TRPV1, one signal is considered a key mechanism. TRPV1 is ubiquitous throughout the nervous system and is a known biomarker of acute and chronic pain sensation and cochlear injury [17]. TRPV1 mRNA expression was significantly enhanced 2-fold compared with the normal group, whereas elevated TRPV1 mRNA level decreased significantly when exposed to RG (Fig. 8B). Furthermore, TrkA is known as a NGF receptor [18], and it also increased following RG treatment (Fig. 8C).

3.9. MAPK activation by RG in AIDN zebrafish

MAPK is related to cell survival and differentiation and is located downstream of the NGF pathway [19,20]. By using Western blotting, we tried to detect any MAPK changes, such as p-MAPK, in the NGF pathway. Western blot analysis showed that p-MAPK in larvae was reduced by alloxan, whereas p-MAPK was significantly elevated in the RG-treated group (Fig. 9).

4. Discussion

Panax ginseng is a traditional oriental medicine that has been used for over 2000 years and has various beneficial effects on the human body [21]. Moreover, RG has been reported to improve hearing loss due to diabetes complications [12]. Diabetes can cause development and progression of sensorineural damage. Some animal models have been established to examine the

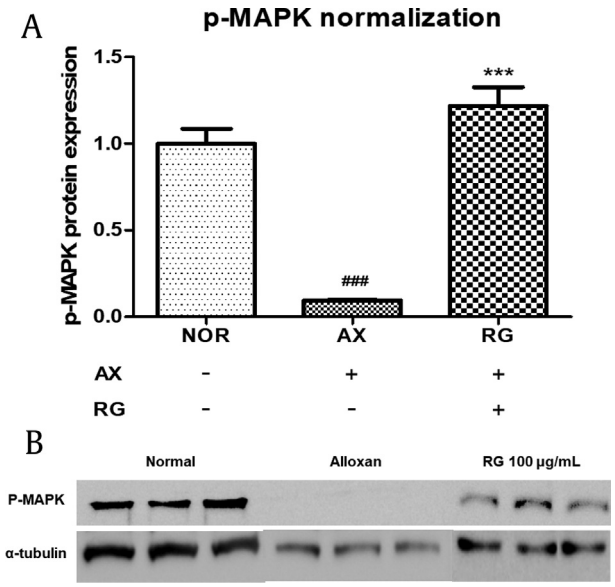

Fig. 9. Expression of p-MAPK in AIDN zebrafish. (A) Normalization of p-MAPK level in zebrafish. (B) Western blot assay of p-MAPK and α-tubulin levels in zebrafish ($^{###}p < 0.001$ compared to normal, $^{***}p < 0.001$ compared to alloxan treatment). AIDN, alloxan-induced diabetic neuromast; p-MAPK, mitogen-activated protein kinase phosphorylation.

therapeutic properties of RG for diabetic subjects, but no zebrafish model has yet been reported [12,22]. To confirm diabetic sensorineural efficacy, we used zebrafish because they offer the advantage of being able to observe neuromast changes in a live model. Therefore, we tried to identify the effect of RG using live zebrafish neuromasts.

First, we established diabetic sensorineural damage in the zebrafish using alloxan, which is a well known experimental diabetogenic agent that causes pancreatic β-cell necrosis leading to a decreased β-cell mass and consequently an inhibition of insulin secretion. Moreover, we previously reported alloxan-induced diabetic zebrafish [27,28]. To establish diabetic sensorineural damage in zebrafish, we confirmed neuromast presence in zebrafish using YO-PRO, which is a fluorescent dye for staining hair cells [23]. Neuromast hair cell death can be easily evaluated by measuring fluorescence loss [24]. The neuromast is a mechanosensory organ, which comprises cranial and trunk neuromasts. Cranial neuromasts are called the anterior lateral line and are present on the head. Trunk neuromasts are called the posterior lateral line and include the neuromasts on the trunk and tail [10,25]. Specifically, we focused on trunk neuromast observation using 0.1% YO-PRO. We determined the optimal alloxan concentration and exposure duration for causing trunk neuromast damage. Trunk neuromasts were observed after exposure to 100 μM, 300 μM, and 500 μM of alloxan for 2 and 4 days. According to our results, alloxan caused hair cell loss in zebrafish neuromasts in a dose- and time-dependent manner. Additionally, the optimal dosage and timing of alloxan exposure for damaged neuromasts in the zebrafish model were 300 μM and 72 hours, respectively. We confirmed that sensitivity of hair cell loss depends on localization of the neuromast. When zebrafish were exposed to alloxan at higher concentrations, the average number of otic hair cells on the head, known as the anterior lateral line, slightly decreased but not significantly so. In contrast, the neuromasts of the posterior lateral line were more sensitive, significantly decreasing in number.

To determine whether alloxan-induced neuromast damage was reduced by RG, zebrafish larvae were treated with RG after alloxan exposure. Our data showed that RG enhanced trunk neuromast recovery after alloxan-induced neuromast damage. Additionally, cilia of neuromast hair cells were severely damaged by alloxan; however, RG stimulated hair cell cilia regeneration, indicating that RG protects the mechanosensitive function of cilia.

We confirmed morphological changes in the hair cells of zebrafish and performed physiological recording to assess functional changes. Alloxan-treated hair cells had a more positive resting membrane potential than normal hair cells. Abnormal movement of ions across the membrane caused by alloxan would result in a charge imbalance across the membrane. On the other hand, the resting membrane potential significantly decreased in the RG-treated group compared to the alloxan-exposed group. We predict that RG protects hair cell function against induced hair cell damage by AIDN. However, the precise mechanism of RG's effect on the resting membrane potential is still not known.

In AIDN zebrafish, pancreatic islet size decreased and recovery was present after treatment with RG. Furthermore, RG stimulated recovery of damaged β-cells and tend to reduce PEPCK expression. It is well known that chronic hyperglycemia, which occurs in diabetes, causes an increase of PEPCK expression [29]; therefore, any agent that diminishes its expression is expected to improve sensorineural damage.

TRPV1 is regulated by NGF and causes a sensation of scalding heat and pain in the peripheral nervous system [30]. TRPV1 expression increased in the AIDN zebrafish but decreased after RG treatment. Also, trkA mRNA level indicated that RG has a nerve-protection effect. The pattern of trkA expression showed that RG has a potential neuron-recovery effect and can help repair diabetic sensorineural damage. NGF stimulates MAPK activation, and our data indicated that MAPK was activated after RG treatment.

In conclusion, we found that RG stimulates neuromast hair cell recovery following damage caused by AIDN. We suggest that the mechanism might be related to the promotion of the NGF pathway through increased expression of TRPV1, trkA, and p-MAPK. Furthermore, RG can improve diabetes symptoms by protecting pancreatic islets and tend to lower PEPCK level. These results suggest that it is possible to treat both diabetes and diabetic sensorineural damage with RG.

Conflicts of interest

The authors have no conflicts of interest to declare.

Acknowledgments

This research was supported by Basic Science Research program through the National Research Foundation of Korea (NRF) funded by the ministry of Education, Science and Technology (NRF-2015R1D1A1A09060469, NRF-2016K1A1A8A01938680).

Abbreviation list

RG	Red ginseng
AIDN	Alloxan-induced diabetic neuromast
SEM	Scanning electron microscopy
NGF	Nerve growth factor
TrkA	Topomyosin receptor kinase A,
MAPK	Mitogen-activated protein kinase,
dpf	Days postfertilization,
hpf	Hours postfertilization,
O1	Otic 1 hair cell
L1	Lateral neuromast 1
L4	Lateral neuromast 4

T	Terminal neuromast
PEPCK	Phosphoenolpyruvate carboxykinase
TRPV1	Transient receptor potential channel vanilloid subfamily type 1

References

[1] Baek KS, Yi YS, Son YJ, Jeong D, Sung NY, Aravinthan A, Kim JH, Cho JY. Comparison of anticancer activities of Korean Red Ginseng-derived fractions. J Ginseng Res 2017;41(3):386–91.

[2] Kim JH, Yi YS, Kim MY, Cho JY. Role of ginsenosides, the main active components of *Panax ginseng*, in inflammatory responses and diseases. J Ginseng Res 2017;41:435–43.

[3] Cheon JM, Kim DI, Kim KS. Insulin sensitivity improvement of fermented Korean Red Ginseng (*Panax ginseng*) mediated by insulin resistance hallmarks in old-aged ob/ob mice. J Ginseng Res 2015;39(4):331–7.

[4] Park TY, Hong M, Sung H, Kim S, Suk KT. Effect of Korean Red Ginseng in chronic liver disease. J Ginseng Res 2017;41:450–5.

[5] Faucherre A, Pujol-Martí J, Kawakami K, López-Schier H. Afferent neurons of the zebrafish lateral line are strict selectors of hair-cell orientation. PLoS One 2009;4(2):e4477.

[6] Santos F, MacDonald G, Rubel EW, Raible DW. Lateral line hair cell maturation is a determinant of aminoglycoside susceptibility in zebrafish (*Danio rerio*). Hear Res 2006;213(1):25–33.

[7] McHenry MJ, Feitl KE, Strother JA, Van Trump WJ. Larval zebrafish rapidly sense the water flow of a predator's strike. Biol Lett 2009;5(4):477–9.

[8] Metcalfe WK, Kimmel CB, Schabtach E. Anatomy of the posterior lateral line system in young larvae of the zebrafish. J Comp Neurol 1985;233(3):377–89.

[9] Raible DW, Kruse GJ. Organization of the lateral line system in embryonic zebrafish. J Comp Neurol 2000;421:189–98.

[10] Gompel N, Cubedo N, Thisse C, Thisse B, Dambly-Chaudière C, Ghysen A. Pattern formation in the lateral line of zebrafish. Mech Dev 2001;105:69–77.

[11] Ghysen A, Dambly-Chaudière C. The lateral line microcosmos. Genes Dev 2007;21:2118–30.

[12] Hong BN, Ji MG, Kang TH. The efficacy of red ginseng in type 1 and type 2 diabetes in animals. Evid Based Complement Alternat Med 2013;2013:593181.

[13] Szkudelski T. The mechanism of alloxan and streptozotocin action in B cells of the rat pancreas. Physiol Res 2001;50(6):537–46.

[14] Radenković M, Stojanović M, Prostran M. Experimental diabetes induced by alloxan and streptozotocin: the current state of the art. J Pharmacol Toxicol Methods 2016;78:13–31.

[15] Livak KJ, Schmittgen TD. Analysis of relative gene expression data using real-time quantitative PCR and the 2(-Delta Delta C(T)) Method. Methods 2001;25(4):402–8.

[16] Elo B, Villano CM, Govorko D, White LA. Larval zebrafish as a model for glucose metabolism: expression of phosphoenolpyruvate carboxykinase as a marker for exposure to anti-diabetic compounds. J Mol Endocrinol 2007;38(4):433–40.

[17] Bauer CA, Brozoski TJ, Myers KS. Acoustic injury and TRPV1 expression in the cochlear spiral ganglion. Int Tinnitus J 2007;13(1):21.

[18] Patapoutian A, Reichardt LF. Trk receptors: mediators of neurotrophin action. Curr Opin Neurobiol 2001;11(3):272–80.

[19] Nguyen TL, Kim CK, Cho JH, Lee KH, Ahn JY. Neuroprotection signaling pathway of nerve growth factor and brain-derived neurotrophic factor against staurosporine induced apoptosis in hippocampal H19-7 cells. Exp Mol Med 2010;42(8):583–95.

[20] Kao SC, Jaiswal RK, Kolch W, Landreth GE. Identification of the mechanisms regulating the differential activation of the mapk cascade by epidermal growth factor and nerve growth factor in PC12 cells. J Biol Chem 2001;276(21):18169–77.

[21] Kim CS, Park JB, Kim KJ, Chang SJ, Ryoo SW, Jeon BH. Effect of Korea red ginseng on cerebral blood flow and superoxide production. Acta Pharmacol Sin 2002;23(12):1152–6.

[22] Quan HY, Kim DY, Chung SH. Korean red ginseng extract alleviates advanced glycation end product-mediated renal injury. J Ginseng Res 2013;37(2):187–93.

[23] Ou HC, Raible DW, Rubel EW. Cisplatin-induced hair cell loss in zebrafish (*Danio rerio*) lateral line. Hear Res 2007;233(1):46–53.

[24] Shin YS, Hwang HS, Kang SU, Chang JW, Oh YT, Kim CH. Inhibition of p38 mitogen-activated protein kinase ameliorates radiation-induced ototoxicity in zebrafish and cochlea-derived cell lines. Neurotoxicology 2014;40:111–22.

[25] Van Trump WJ, McHenry MJ. The morphology and mechanical sensitivity of lateral line receptors in zebrafish larvae (*Danio rerio*). J Exp Biol 2008;211(13):2105–15.

[26] Zhu Y, Colak T, Shenoy M, Liu L, Pai R, Li C, Mehta K, Pasricha PJ. Nerve growth factor modulates TRPV1 expression and function and mediates pain in chronic pancreatitis. Gastroenterology 2011;141(1):370–7.

[27] Nam YH, Hong BN, Rodriguez I, Ji MG, Kim K, Kim UJ, Kang TH. Synergistic potentials of coffee on injured pancreatic islets and insulin action via KATP channel blocking in zebrafish. J Agric Food Chem 2015;63(23):5612–21.

[28] Nam YH, Le HT, Rodriguez I, Kim EY, Kim K, Jeong SY, Woo SH, Lee YR, Castañeda R, Hong J, et al. Enhanced antidiabetic efficacy and safety of compound K⁄ β-cyclodextrin inclusion complex in zebrafish. J Ginseng Res 2017;41(1):103–12.

[29] Shao J, Qiao L, Janssen RC, Pagliassotti M, Friedman JE. Chronic hyperglycemia enhances PEPCK gene expression and hepatocellular glucose production via elevated liver activating protein/liver inhibitory protein ratio. Diabetes 2005;54(4):976–84.

[30] Lauria G, Morbin M, Lombardi R, Capobianco R, Camozzi F, Pareyson D, Manconi M, Geppetti P. Expression of capsaicin receptor immunoreactivity in human peripheral nervous system and in painful neuropathies. J Peripher Nerv Syst 2006;11(3):262–71.

[31] Apfel SC. Nerve growth factor for the treatment of diabetic neuropathy: what went wrong, what went right, and what does the future hold? Int Revi Neurobiol 2002;50:393–413.

[32] Pittenger G, Vinik A. Nerve growth factor and diabetic neuropathy. Exp Diabetes Res 2003;4(4):271–85.

[33] Hirose M, Kuroda Y, Murata E. NGF/TrkA signaling as a therapeutic target for pain. Pain Pract 2016;16(2):175–82.

[34] Khan N, Smith MT. Neurotrophins and neuropathic pain: role in pathobiology. Molecules 2015;20(6):10657–88.